Article

Structure of Zone-Cast HBC–CH Films

Dag W. Breiby, Oliver Bunk, Wojciech Pisula, Theis I. Slling,
Adam Tracz, Tadeusz Pakula, Klaus Mllen, and Martin M. Nielsen

J. Am. Chem. Soc., **2005**, 127 (32), 11288-11293• DOI: 10.1021/ja042355e • Publication Date (Web): 21 July 2005

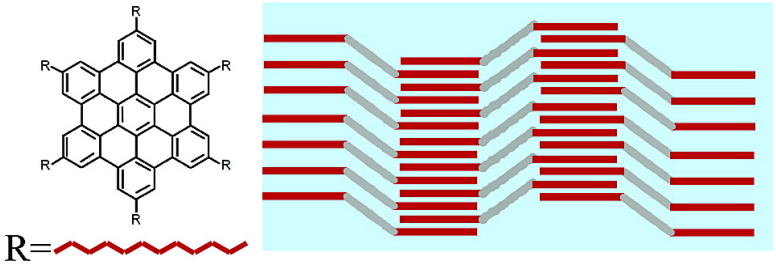

J|A|C|S
ARTICLES
Published on Web 07/21/2005

Structure of Zone-Cast HBC−$C_{12}H_{25}$ Films

Dag W. Breiby,*,† Oliver Bunk,‡ Wojciech Pisula,§ Theis I. Sølling,|| Adam Tracz,⊥ Tadeusz Pakula,§ Klaus Müllen,§ and Martin M. Nielsen†

Contribution from the Danish Polymer Centre, Risø National Laboratory, P.O. Box 49, 4000 Roskilde, Denmark, Paul Scherrer Institute, 5232 Villigen PSI, Switzerland, Max-Planck-Institute for Polymer Research, Ackermannweg 10, D-55128 Mainz, Germany, Department of Chemistry, University of Copenhagen, Universitetsparken 5, 2100 Copenhagen, Denmark, and Centre of Molecular and Macromolecular Studies, Polish Academy of Sciences, 90-363 Łodź, Sienkiewicza 112, Poland

Received December 20, 2004; E-mail: dag.werner.breiby@risoe.dk

Abstract: The structure of a thin zone-cast film of the hexa-*n*-dodecyl-substituted hexa-*peri*-benzocoronene (HBC) has been investigated using grazing incidence X-ray diffraction. A model with an orthorhombic unit cell containing two molecules accounts well for the observations. The molecules are arranged in a "herringbone" structure resembling the packing observed for unsubstituted HBC. The molecular disk planes are oriented perpendicularly to the substrate, rotated by approximately 39° about the film normal. The relatively long side chains of dodecyl were found to be in an ordered interdigitated state. The aliphatic side chains and the aromatic HBC-cores segregate to form regular vertical domains spanning the film thickness. For in-plane rocking scans a discrete orientation distribution is observed with peaks at regular angle intervals. We interpret this as a grain boundary effect induced by alkyl chain stacking faults.

Introduction

The prospects of organic electronics are promising, with an important goal being to make cheap plastic sensors and circuits.[1] The importance of well-defined molecular order to exploit the highly anisotropic properties of the specifically designed molecules is well recognized.[2,3] A requirement for high mobility in films of organic conjugated molecules is a good overlap of the π electrons of neighboring molecules. Many pathways have been explored to achieve highly connected networks of $\pi-\pi$ interacting molecules, ranging from modifications of the chemical structure to the choice of processing methods including spin casting, drop casting, and molecular vapor deposition.

Hexa-peri-benzocoronenes (HBC), see structure 1, are graphenes of well-defined size and shape.[4] Graphenes are rich in π electrons, and one might thus expect a high degree of overlap between adjacent π orbitals. It appears that, in most reported organic thin film structures of planar molecules, the molecules tend to be oriented vertically, i.e., "edge on" with respect to the substrate.[2−8] Pure HBC is highly crystalline and poorly soluble. Because of electrostatic quadrupolar interactions, these molecules tend to pack in the so-called herringbone structure.

Chemical modification of organic molecules, notably by side-chain substituents, allows tailoring their physiochemical properties, including the desired self-assembly behavior. For many organic molecules and polymers, substituting with (typically alkyl) side chains renders the molecules solution processable without strongly perturbing the electronic properties of the core molecule. As might be anticipated for alkyl-substituted HBC having electron-rich planar cores, these disk-shaped molecules tend to microsegregate into columns of stacked aromatic cores. These stacks are sometimes described as highly conducting "molecular wires", kept separated by the electronically inactive alkyl side chains. Mobilities up to 1.0 cm^2/Vs have been reported for HBC derivatives.[7]

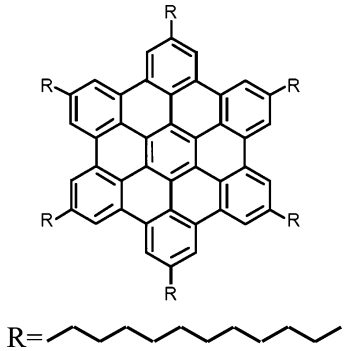

structure 1

The packing motif of "discotics" can be manipulated by the film-casting technique. For example, epitaxial growth on poly-

† Risø National Laboratory.
‡ Paul Scherrer Institute.
§ Max-Planck-Institute for Polymer Research.
|| University of Copenhagen.
⊥ Polish Academy of Sciences.

(1) *Semiconducting Polymers: Chemistry, Physics and Engineering*; Hadziioannou, G., van Hutten, P. F., Eds.; Wiley: Weinheim, 2000.
(2) Samuelsen, E. J.; Aasmundtveit, K. E.; Breiby, D. W. In *Electronic and Optical Properties of Conjugated Molecular Systems in Condensed Phases*; Hotta, S., Ed.; Research Signpost: Kerala, India, 2003.
(3) Sirringhaus, H. et al. *Nature* **1999**, *401*, 685−688.
(4) Tracz, A.; Jeszka, J. K.; Watson, M. D.; Pisula, W.; Müllen, K.; Pakula, T. *J. Am. Chem. Soc.* **2003**, *125*, 1682−1683.
(5) Aasmundtveit, K. E. et al. *Macromolecules* **2000**, *33*, 3120−3127.

10.1021/ja042355e CCC: $30.25

(tetrafluoroethylene) alignment layers has been reported for HBC−$C_{8,2}$ cast from solution.[9,10] For film processing, we employed zone casting,[11] a technique first reported in the early 1980s,[12] but it has not been widely used until recently.[4,11] Basically, this technique consists of continuously supplying a heated solution of the molecules through a nozzle onto a substrate that is slowly and continuously translated with respect to the nozzle. By tuning the deposition speed, stationary solidification conditions are obtained at the moving meniscus where the solution gets in contact with the substrate. The result is a highly directional drying front, giving nucleation and directed crystalline growth. Thereby, a high degree of in-plane alignment can be achieved *without* using any aligning substrate, stretching, or rubbing.

The surface-sensitive technique of grazing incidence X-ray diffraction (GID) was used for characterizing the films. The zone-cast films were found to have a complex, yet highly reproducible, crystalline structure. An unusually high degree of biaxial orientation was observed, implying that these polycrystalline thin films effectively resemble single crystals, where also the alkyl side chains are in a well-defined stacking arrangement.

Experimental Results

The Films. The organic material HBC−$C_{12}H_{25}$ was synthesized as published previously.[13] The zone-cast films were found to be thin and homogeneous. The thickness has been estimated to about 150 Å by atomic force microscopy (AFM) measurements.[11] The films were transparent and could hardly be observed by the naked eye. Because of a corrugated surface, X-ray reflectometry did not yield any estimate of the film thickness, see later. The film structure is highly reproducible, as evidenced by the many films studied at different beamtime sessions, always exhibiting the same peak positions and relative intensities.

The Main Structural Features. GID studies are performed with the beam impinging onto the sample surface at a grazing incidence angle (here, 0.16°), being near the critical angle for total reflection from the organic film surface. As a result, the (background) scattering from the substrate is strongly suppressed, effectively enhancing the signal from the thin organic film.[14,15]

The scattering vector **Q** was decomposed into components Q_x, Q_y, and Q_z, with Q_z oriented along the film normal. The in-plane components Q_x and Q_y were chosen to be perpendicular and parallel to the columns, respectively. The repetition distance d is related to Q by $d = 2\pi/Q$, and $Q^2 = Q_x^2 + Q_y^2 + Q_z^2$. Figure 1 shows a cross section of reciprocal space corresponding to the "equatorial" plane being perpendicular to the molecular stacks (i.e., $Q_y = 0$). It was obtained by doing repeated Q_x scans for increasing Q_z values using a point detector. The many higher orders are evidence for a well-ordered structure. The molecules are evidently highly biaxially oriented, as judged by the sharp peaks found in both the Q_xQ_y and the Q_xQ_z planes.

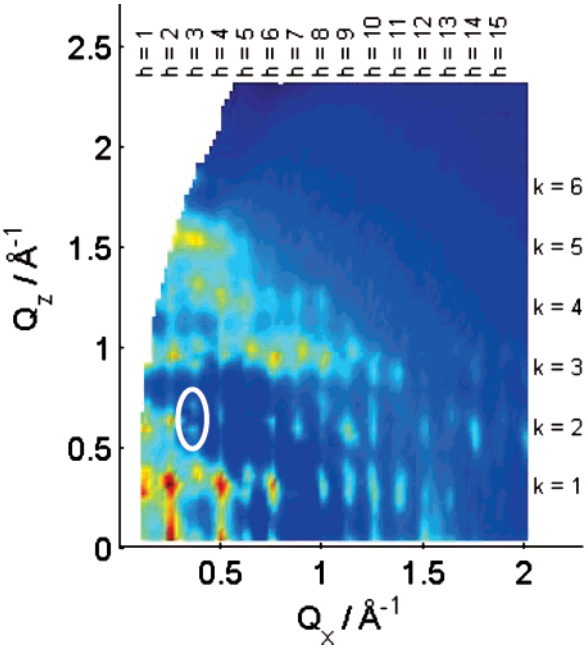

Figure 1. Picture of the Q_xQ_z plane for $Q_y = 0$, obtained by doing repeated scans with the point detector. The step lengths were 0.02 and 0.04 Å^{-1} in the Q_x direction and Q_z directions, respectively. The "forbidden" region near the Q_z axis cannot be reached by the GID technique. This kind of picture cannot be obtained using, e.g., an area detector because the sample orientation differs for different reflections. The vertical streaks are crystal truncation rods. h and k denote Miller indices; l is 0. Note the many higher order mixed index diffraction peaks, demonstrating a high degree of crystalline order. The ellipse highlights an example of a peak splitted in the Q_z direction.

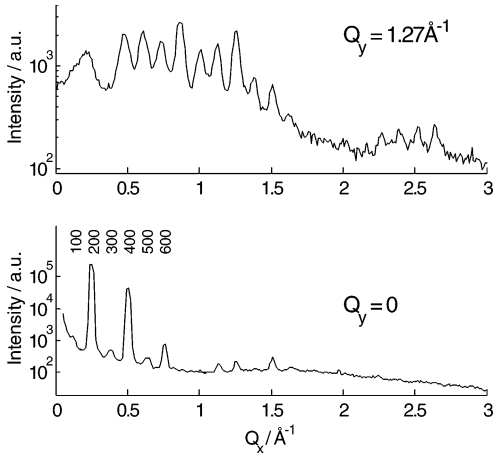

Figure 2. In-plane results ($Q_z \approx 0$). The $Q_y = 0$ ("equatorial") scan corresponds to $l = 0$. Note the logarithmic intensity scale; the peaks are very intense. The alternating weak and strong peaks are due to the face centered unit cell. For $Q_y = 1.27$ Å^{-1} ($l = 1$), several strong peaks are clustered around $Q_x \approx 1$ Å^{-1}.

The closely spaced peaks in the Q_x direction correspond to the intercolumnar distance of about 24.5 Å. If scanning in the Q_y direction (not shown), the only peaks are at multiples of 1.27 Å^{-1}, yielding an intracolumnar stack spacing between adjacent molecules of 4.96 Å. The pattern of weak and strong reflections gives important information about the contents of the unit cell, as modeled later.

In-plane results of Q_x scans for $Q_y = 0$ and for $Q_y = 1.27$ Å^{-1} are shown in Figure 2. The $Q_y = 0$ line is of course similar to the $k = 0$ row of reflections in Figure 1. Note also the strong group of reflections at $Q_x \approx Q_y \approx 1.27$ Å^{-1}, which we attribute to a tilt of the disk-shaped

(6) Wackerbarth, H.; Grubb, M.; Zhang, J. D.; Hansen, A. G.; Ulstrup, J. *Angew. Chem., Int. Ed.* **2004**, *43*, 198−203.
(7) van de Craats, A. M.; Warman J. M. *Adv. Mater.* **2001**, *13*, 130−133.
(8) Breiby, D. W.; Samuelsen, E. J.; Konovalov, O.; Struth, B. *Langmuir* **2004**, *20*, 4116−4123.
(9) Bunk, O.; Nielsen, M. M.; Solling, T. I.; van de Craats, A. M.; Stutzmann, N. *J. Am. Chem. Soc.* **2003**, *125*, 2252−2258.
(10) van de Craats, A. M.; Stutzmann, N.; Bunk, O.; Nielsen, M. M.; Watson, M.; Müllen, K.; Chanzy, H. D.; Sirringhaus, H.; Friend, R. H. *Adv. Mater.* **2003**, *15*, 495−499.
(11) Pisula, W.; Menon, A.; Stepputat, M.; Lieberwirth, I.; Kolb, U.; Tracz A.; Sirringhaus, H.; Pakula, T.; Müllen, K. *Adv. Mater.* **2005**, *17*, 684−689.
(12) Burda, L.; Tracz, A.; Pakula, T.; Ulanski, J.; Kryszewski, M. *J. Phys. D: Appl. Phys.* **1983**, *16*, 1737−1740.
(13) Ito, S.; Wehmeier, M.; Brand, J. D. Kübel, C.; Epsch, R.; Rabe, J. P.; Müllen, K. *Chem.−Eur. J.* **2000**, *6*, 4327−4342.
(14) Bunk, O.; Nielsen M. M. *J. Appl. Cryst.* **2004**, *37*, 216−222.
(15) Als-Nielsen, J.; McMorrow, D. *Modern X-ray Physics*; John Wiley & Sons, Ltd.: West Sussex, 2004.

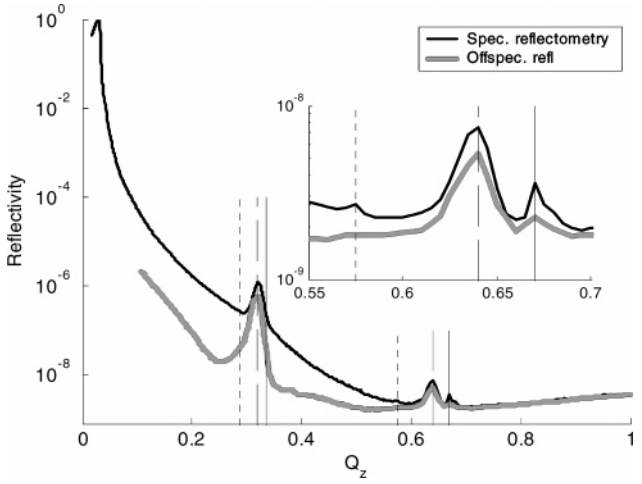

Figure 3. Reflectometry scans plotted as function of Q_z are shown. The off-specular scan was performed with a slight offset $Q_x \neq 0$. No thickness fringes are seen, suggesting a corrugated surface of the film. The strong peak at $Q_z = 0.320$ Å^{-1} corresponds to a 19.6-Å characteristic distance. Vertical lines are at $Q_z = \{0.288, 0.320, 0.335\}$ Å^{-1} and their second harmonic. The inset shows a magnified view of the structure around the second-order peaks. The peaks are due to crystallites (not thickness), and they thus appear more pronounced in the off-specular geometry, where the Fresnel-reflected intensity is negligible.

molecules. The intensities are in full agreement with qualitative electron diffraction data of the same material cast on amorphous graphite, ref 11. This is somewhat surprising taking into account both the different nature of these diffraction techniques and that films cast on differing substrates are being compared.

A specular scan (**Q** perpendicular to the sample substrate, $Q_x = Q_y = 0$) is given in Figure 3. The absence of thickness fringes is interpreted as being due to considerable surface corrugation. The peak at $Q_z \approx 0.3$Å^{-1} is a composite of three contributions, with the most pronounced being at $Q = 0.32$ Å^{-1}, giving $d = 19.6$ Å.

The abovementioned observations can be accounted for by an orthorhombic unit cell, having cell parameters $a = 49.4$ Å, $b = 19.6$ Å, and $c = 4.96$ Å. We define the *h00* reflections to be on the Q_x axis, *00l* on the Q_y axis, and *0k0* on the Q_z axis. With two molecules per unit cell, this gives a density of 1.06 g/cm^3, which is common for organic materials.

The degree of in-plane orientation is usually measured by scanning φ ("rocking scans") for fixed detector positions. However, by doing repeated linear scans and synthesizing a picture, a much better impression of the structure is obtained, as demonstrated in Figure 4. The rocking curve peak shape is often Gaussian due to the (normal) distribution expected for a distribution containing many crystallites.[16] In the present atypical case, the (intercolumnar) *h00* reflections are seen to be distributed with one main orientation along Q_x, i.e., perpendicular to the zone-casting direction. The on-axis rocking peaks are indeed narrow, with a full width at half maximum in φ of about 1°, which implies a high degree of alignment. However, rather than being single peaks (with 180° periodicity) in φ, also much weaker peaks of approximately the same $|\mathbf{Q}|$ are seen at discrete angles with $\Delta\varphi \approx 9°$. Note that the intensities in Figure 4 are on a logarithmic scale. This feature has not been observed with electron diffraction,[11] presumably because the off-axis peaks are much weaker than the other peaks. In addition to yielding more quantitative results, an additional advantage of GID as compared with electron diffraction is the feasibility of measuring out-of-plane reflections.

Simulations

To obtain structural information beyond the unit cell, structure factor simulations were carried out as described in the Experimental Section. An important simplification was the use of so-called rigid-body optimizations, i.e., the HBC cores (and when included, also the side chains) were not allowed to bend or twist. The graphenes were parametrized as a planar sheet with a carbon−carbon distance of 1.415 Å. For a unit cell with two molecules, this reduces the number of free parameters to a total of 9, i.e., 3 Euler angles for describing the orientation of the first molecule, and (3 + 3) parameters for modeling the displacement and the orientation of the second molecule with respect to the first.

Within the constraints of an orthogonal unit cell with known dimensions and a rigid body description of the molecules, we tried many qualitatively different molecular arrangements. Also crystal structures with both HBC cores tilted in the same direction were explored, without obtaining adequate fits. It was also attempted to use a trial cell with doubled or even tripled volume to give more possibilities for molecular orientations. The figure of merit was estimated by visual inspection of the fits and by χ^2 deviations from the experimental scans.

The first simulations were done with the additional assumption that most of the coherently scattered intensity originated from the aromatic HBC cores. For modeling the diffraction patterns, this rough assumption of neglecting the side chains worked rather well. The only satisfactory model obtained was with a herringbone-packing motif, having about 16.5 Å void between the HBC stacks.

An interesting point is that the structure resembles the herringbone structure found in unsubstituted HBC, with every other stack shifted by $c/2$ (2.48 Å) in the c direction. Instead of orienting with the disk normal in the stacking direction, the molecules were found to be rotated about the sample normal by $\sim 40 \pm 2°$. This tilt is about a vertical axis; no evidence was found for an out-of-plane component of the disk normals.

By consideration of the schematic in Figure 5a, it appears that a plausible packing of the side chains is to be oriented parallel to the a axis. As can be inferred from the figure, the space between columns in the a direction corresponds to the estimated length of an extended dodecane molecule, i.e., about 16 Å. The structure factor simulations provide further evidence that rather than forming a disordered "halo" around the HBC cores; the side chains are predominantly orienting parallel to the substrate and perpendicularly to the stacking direction. By including idealized straight dodecyl chains in the simulations, all being oriented along a and attached to their proper positions along the HBC perimeter, the χ^2 estimator used for the goodness of fit was improved by ~30%. The extended side chains are thus expected to form a rather regular lattice in the *bc* plane, cf. Figure 5.

The simplest structural model consistent with the data is presented in Figure 5. A corresponding simulation for the $k = 0$, $l = -1$ reflections is shown in Figure 6. The simulated intensities are seen to be in fair agreement with the experimental data. Note that the presented simulation is for a well-defined line in reciprocal space, it should not be confused with a powder diffraction scan averaging over all directions. A considerable uncertainty is related to the background scattering. An important part of this scattering is from the amorphous substrate, which is only partly accounted for in Figure 6. Therefore, a full agreement between data and simulations should not necessarily

(16) Breiby, D. W.; Samuelsen, E. J. *J. Polym. Sci. B: Polym. Phys.* **2003**, *41*, 3011−3025.

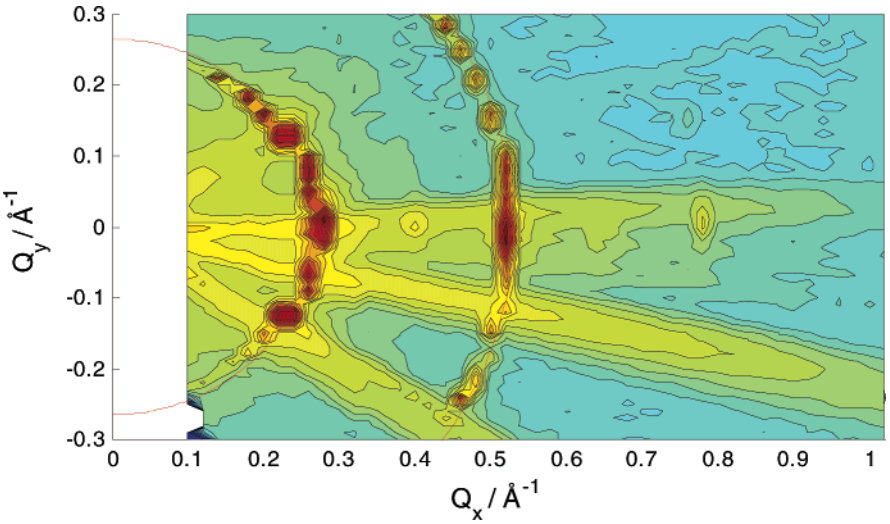

Figure 4. In-plane intensity map ($Q_z \approx 0$), with the intensity being on a logarithmic scale. The map was obtained by repeated scans, with step lengths 0.02 and 0.01 Å^{-1} in the Q_x and Q_y directions, respectively. The circle segments, corresponding to the *200* and *400* reflections, emphasize that these peaks have approximately the same Q value. They exhibit an exotic orientational distribution, where the crystallites are only allowed to assume certain angles with respect to each other. The radial streaks are not understood. The feature in the lower left corner is an artifact. The slight asymmetry in intensities might be due to nonperfect sample line up.

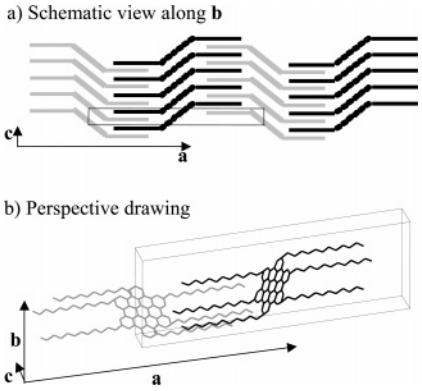

Figure 5. Illustrations of the molecular packing and the unit cell. (a) A projection along the *b* axis emphasizing the tilted molecules in the herringbone packing. The side chains, oriented along *a*, are indicated schematically with straight lines. The distance between the HBC stacks is about 16.5 Å, which corresponds to the length of an extended dodecyl chain. For readability, every other stack is gray and black. (b) The idealized unit cell drawn in perspective. In reality, the side chains are probably somewhat more disordered, filling the volume of the unit cell.

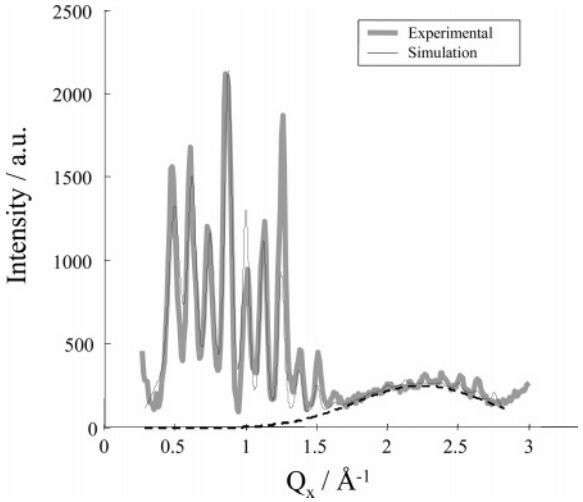

Figure 6. The experimental curve is for $Q_y = 1.27$ Å^{-1}, $Q_z = 0.03$ Å^{-1}. The simulated curve fits the experimental data well. A Gaussian curve was imposed as a background centered at $Q_x \approx 2.3$ Å^{-1} (broken line), accounting for the attenuated scattering from the amorphous glass substrate.

be expected, and we judge that a more detailed modeling of the structure will not be fruitful.

Discussion

Structure and Side-Chain Packing. The fact that there is long-range order between the columns, at least 15 higher order reflections can be seen in Figures 1 and 2, is remarkable in view of the high volume fraction of relatively long dodecyl side chains. That structural information is mediated between the aromatic stacks implies that the alkyl chains must be in a highly ordered state. Thus, despite the fact that dodecane is a liquid at room temperature ($T_m = -9.65$ °C), the dodecyl side chains are in a stabilized frozen state when anchored to the comparably heavy and structurally stiff HBC cores. In the crystalline state, the side chains will have a certain mobility but not as high as in the liquid crystalline phase reached at higher temperatures. Differential scanning calorimetry shows a weak endothermic peak at ~42 °C,[17] which we interpret as an increase of alkyl chain mobility.

A crystallographic distance of 4.96 Å and a tilt angle of 40° yield a $\pi-\pi$ stacking distance of 3.8 Å between adjacent HBC molecules. Compared with the "standard" value reported for π stacking, being about 3.5 Å, this value appears somewhat high. Part of the reason for this discrepancy might be uncertainty in the modeled orientation angles of the HBC cores. A 45° tilt angle yields 3.5 Å, but at the cost of a significantly reduced goodness of fit. An example of close-packed hydrocarbons is high-density polyethylene, which has an orthorhombic unit cell with $a = 7.41$ Å and $b = 4.92$ Å. The two polymer chains per unit cell orient along the *c* axis, having $c = 2.54$ Å.[18] This gives a chain density per area of $2/(7.41 \times 4.92)$ Å^{-2} = 0.055 Å^{-2}. The present case, assuming six interdigitating chains, gives a density of $6/(19.6 \times 4.96)$ Å^{-2} = 0.062 Å^{-2}, being about 13% higher. One might thus speculate that the observed structure is

(17) Fischbach, I.; Pakula, T.; Minkin, P.; Fechtenkotter, A.; Müllen, K.; Spiess, H. W.; Saalwachter, K. *J. Phys. Chem. B* **2002**, *25*, 6408−6418.
(18) Swan, P. R. *J. Polym. Sci.* **1962**, *56*, 403−407.

a compromise between the alkyl chains desiring less dense packing and that the HBC cores trying to organize more densely to have a spacing closer to 3.5 Å.

With the evidence for ordered interdigitated side-chain packing, we conjecture that the observed discrete azimuth orientation distribution, cf. Figure 4, can be ascribed to a mismatch (local stacking fault) between the alkyl chains of adjacent molecules. Such a stacking mismatch has been reported, e.g., for alkyl chains in Langmuir films.[19] As an estimate, with 4.96 Å between the alkyl chains, a stacking error inducing a shift of 2.54 Å (the C−C−C distance in hydrocarbon chains) gives an off-axis angle $\varphi' = \tan^{-1}(2.54/4.96) \approx 27°$. This is indeed close to the strongest off-axis peak for the 200 distribution, being at 28°, cf. Figure 4.

Grain boundaries are an important, yet undesired, feature of organic films, known to limit the charge mobility. To the best of our knowledge, similar grain orientations in organic materials have not previously been published. We have found indications that thermal annealing increases the intensity of the off-axis peaks. Further details relating to thermal annealing will be published elsewhere. One might suggest as an alternative hypothesis that this mechanism of a "locked-in" shift occurs between adjacent HBC cores rather than between the side chains, which would yield a similar orientation effect. However, because the π-stacking system is arguably stiffer than the crystalline side-chain packing, we conjecture that the packing faults are induced by the side chains.

An unresolved issue is related to the finer details of Figures 1 and 3, namely, the finer splitting of the peaks. For instance, for $h = 3$ and $k = 2$ in Figure 1, it is readily seen that the peak is split. This splitting can also be seen in the reflectometry scans, cf. Figure 3. This may be evidence for several phases, as a motif of three related peaks occurs repeatedly. It has been reported previously that three different domains are observed at the surface of a zone cast HBC−C_{12} film using AFM.[4] The authors of that study speculate that this might be due to (i) a unique unit cell with different orientations, (ii) surface reconstruction, or (iii) polymorphism. With our new results, we can exclude (i) as none of the three distances observed in Figure 3 are equal to *a* or *b*. Because surface reconstructions do not give any periodicity perpendicularly to the substrate, the only remaining explanation is polymorphism.

An interesting aspect of the crystalline structure is that it appears that the material has microsegregated into vertical ABAB... lamellae or "stripes". The "A" domains are approximately 16 Å wide containing the aliphatic side chains, and the "B" domains are about 9 Å of aromatic HBC stacks. This structure can be considered a compromise between alkyl chain packing and the preferred herringbone stacking of the aromatic disks. We conjecture that with a proper choice of solvent, the aliphatic packing can be dissolved while preserving ordered π stacks of the HBC cores. The present work suggests an intuitive structural explanation for the fact that the slightly modified molecule of HBC−phenyl-C_{12} is a liquid crystal.[17] The phenyl rings prevent the hydrocarbon chains from packing densely.

By comparison of the unit cell "height" *b* of 19.6 Å with the film thickness being about 150 Å, it is likely that the crystallites span the entire film thickness. As a consequence, one might expect also the top surface of the film to have regular stripes of alternating chemistry. Clearly, this invites further studies, not only of the communication between adjacent HBC core molecules in the vertical direction but also of the potential use of the films as a nanopatterned surface.

Structure Factor Considerations. The simulations in Figure 6 illuminate the effect of the structure factor for stacked organic molecules with a pronounced disk shape (high aspect ratio). For tilted molecules, the crystallographic repetition distance along the stacks differs from the $\pi-\pi$ interaction distance, i.e., the shortest distance, between the planar molecules. The tilt of the disks reduces the structure factor $|F|^2$ in the crystallographic (here, Q_y) direction. Conversely, the tilted (yet parallel) molecules yield a strong modulation of the electron density in directions close to the disk normal. As a consequence, the tilted planar molecules effectively enhance the intensity of the mixed-indexed peaks that happen to be in the appropriate direction. It is seen from Figure 2 that the *h0−1* reflections having $0.5 < Q_x < 1.5$ Å^{-1} are much stronger than the others. As $Q_y \approx 1.27$ Å^{-1} for these peaks, one thus has an intuitive physical explanation for the molecular tilt, as modeled more rigorously by the simulations.

Because of the 6-fold (high) rotational symmetry of the HBC cores, the diffraction patterns are not particularly sensitive to rotations about the molecular normal. The best fit we obtained was for one of the two molecules in the unit cell having a "flat edge" parallel to the substrate, and the other being rotated about its disk normal by about 15° from that orientation. However, because of the discussed experimental uncertainty of the structure factors, these values might not be reliable.

Many films of discotic molecules exhibit a comparably low or moderate degree of order, yielding only a few diffraction peaks. It is then sometimes difficult to judge whether the structure resembles the herringbone ordering having pairwise columns with opposite tilts or rather has all molecules within a crystallite tilted in the same direction (effectively a single-collumn arrangement). In the latter case, other crystallites will have the (thermodynamically equivalent) structure with the opposite tilt. As, e.g., HBC molecules are highly birefringent, absence of optical (UV−vis) anisotropy is sometimes interpreted as being due to a herringbone arrangement. Because the crystalline domains tend to be smaller than the resolution of optical measurements this is not really a rigorous test. The demonstration that a single-column unit cell cannot be the case for HBC−C_{12} films is another important contribution from this work.

Conclusions

By use of GID, the structure of zone-cast HBC−C_{12} has been investigated in detail. More than 15 orders of diffraction are seen for some of the reflections, revealing that the films are highly crystalline and have a well-defined biaxial orientation. An orthorhombic unit cell containing two molecules accounts well for the observed features. From structure factor simulations it was found that the HBC cores orient "edge on" with respect to the substrate. The disks assume a herringbone-packing motif, with opposite rotations of $39 \pm 2°$ between neighboring stacked columns.

The observation of extraordinarily high crystalline order implies that the commonly used assumption of disordered side

(19) Bjørnholm, T.; Hassenkam, T.; Reitzel, N. *J. Mater. Chem.* **1999**, *9*, 1975−1990.

chains appears not to hold in the present case. Structure factor simulations suggest that the side chains orient in an extended fashion perpendicularly to the application direction. High crystalline order of the side chains is in fact a requirement to account for the observed high co-registry of the stacks. The discovery of weaker rocking peaks at discrete rotation angles is interpreted as a grain boundary effect. Apparently, the discrete angles can be understood in terms of "stacking faults" of the side chains, giving an offset of one CH_2 unit between neighboring molecules.

This work has several implications for improving the performance of organic thin film devices. Knowing the detailed structure is crucial information for modeling the molecular properties. We have demonstrated the importance of carefully designed processing in general and the ability of zone casting for obtaining films with an outstanding degree of order in particular.

Acknowledgment. We thank the HASYLAB team for technical assistance. DanSync and the Danish Technical Research Council are gratefully acknowledged for financial support.

Supporting Information Available: Experimental Section and complete refs 3 and 5. This material is available free of charge via the Internet at http://pubs.acs.org.

JA042355E